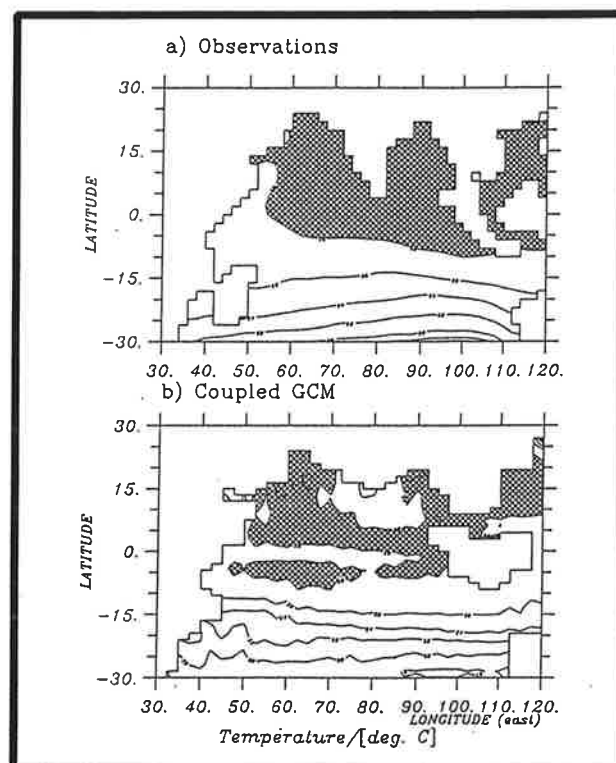




# Max-Planck-Institut für Meteorologie

## REPORT No. 104



## CLIMATE VARIABILITY IN A COUPLED GCM PART II: THE INDIAN OCEAN AND MONSOON

by

MOJIB LATIF • ANDREAS STERL • MICHEL ASSENBAUM  
MARTINA M. JUNGE • ERNST MAIER-REIMER

HAMBURG, APRIL 1993

AUTHORS:

Mojib Latif  
Michel Assenbaum  
Martina M. Junge  
Ernst Maier-Reimer

Max-Planck-Institut  
für Meteorologie

Andreas Sterl

KNMI  
Postbus 201  
NL-3730 AE de Bilt  
The Netherlands

MAX-PLANCK-INSTITUT  
FÜR METEOROLOGIE  
BUNDESSTRASSE 55  
D-2000 HAMBURG 13  
F.R. GERMANY

Tel.: +49 (40) 4 11 73-0  
Telex: 211092mpime d  
Telemail: MPI.METEOROLOGY  
Telefax: +49 (40) 4 11 73-298

# CLIMATE VARIABILITY IN A COUPLED GCM PART II: THE INDIAN OCEAN AND MONSOON

M. Latif, A. Sterl<sup>\*)</sup>, M. Assenbaum, M. M. Junge, and E. Maier-Reimer

Max-Planck-Institut für Meteorologie  
Bundesstr. 55, D-2000 Hamburg 13  
Germany

<sup>\*)</sup>Present affiliation: KNMI, Postbus 201,  
NL-3730 AE de Bilt, The Netherlands

## Abstract

We have investigated the seasonal cycle and the interannual variability of the tropical Indian Ocean circulation and the Indian Summer Monsoon simulated by a coupled ocean-atmosphere general circulation model in a 26 year integration. Although the model exhibits significant climate drift, it simulates realistically the seasonal changes in the tropical Indian Ocean and the onset and evolution of the Indian Summer Monsoon. The amplitudes of the seasonal changes, however, are somewhat underestimated.

The coupled GCM also simulates considerable interannual variability in the tropical Indian Ocean circulation which is partly related to the El Niño/Southern Oscillation (ENSO) phenomenon and the associated changes in the Walker Circulation. Changes in the surface wind stress appear to be crucial in forcing interannual variations in the Indian Ocean SST. As in the Pacific Ocean, the net surface heat flux acts as a negative feedback on the SST anomalies.

The interannual variability in Monsoon rainfall is simulated by the coupled GCM only about half as strongly as observed. This is related to the fact that the simulated interannual variability in the Indian Monsoon is caused by internal processes within the atmosphere only. In contrast, observations show a clear lead-lag relationship between interannual variations in the Monsoon rainfall and tropical Pacific sea surface temperature (SST) anomalies. The atmospheric GCM also fails to reproduce this lead-lag relationship, when run in a stand-alone integration with observed SSTs prescribed. These results indicate that important physical processes relating tropical Pacific SST to Indian Monsoon rainfall are not adequately modelled in our atmospheric GCM.

## 1. Introduction

The climate system in the Indian Ocean/Asian region is characterized by rapid changes on seasonal time scales which are forced by the seasonal variations in the differential heating of the Indian Ocean and the adjacent Asian land masses (Meehl (1992)). This differential heating forces the Monsoon Circulation in the atmosphere which gives rise to the Indian Summer Monsoon rainfall. The seasonal variations in the Monsoon Circulation also drive characteristic circulation patterns in the Indian Ocean. Among those, the annual reversal of the Somali Current and the semi-annual occurrence of an equatorial surface jet, the Wyrski Jet, are the most prominent representatives (Lighthill (1969), Wyrski (1973)).

The Indian Ocean/Asian region has attracted many modeling efforts. Reviews of Indian Ocean modeling can be found, for instance, in Knox and Anderson (1985), Knox (1987), and Luther (1987), and an overview of recent Monsoon modeling activities focussing on the predictability of Monsoon rainfall is given in a workshop report issued by the World Meteorological Organization (WMO (1992)). However, although large-scale air-sea-land interactions are crucial in understanding the climate variability in this part of the world, most modeling studies have been conducted using single component models prescribing boundary conditions from observations. In this paper we describe the climate variability in the Indian Ocean/Asian region simulated by a coupled ocean-atmosphere general circulation model (CGCM). The CGCM, described in detail in Part I of this paper (Latif et al. (1993a), hereafter referred to as Part I), simulates realistically the climate variability in the tropical Pacific, in particular the El Niño/Southern Oscillation (ENSO) phenomenon, and was also applied successfully to ENSO predictions (Latif et al. (1993b)).

Coupled modeling is a rapidly progressing field, because of the large scientific and public interest in predictions of potential anthropogenic climate changes and natural climate variations. Both issues require a proper representation of both the oceanic and the atmospheric circulation. The tropical behaviour of a large number of coupled ocean-atmosphere general circulation models was described recently by Neelin et al. (1992). However, that study was restricted to the tropical Pacific only, because of the predominance of the ENSO phenomenon in the interannual variability of the

tropical climate system. Nevertheless, there are other important scientific questions concerning the tropical climate system for which coupled models are needed. Will, for instance, the Monsoon Circulation and its related typical rainfall patterns change in response to the increased abundance of greenhouse gases in the atmosphere? Or, can we predict the strength of next year's Indian Summer Monsoon or Sahel rainfall?

Before, however, we can answer these and other important questions related to the tropical climate system, we have to verify the coupled models, since they generally suffer from climate drift even when the individual model components give realistic results when forced by observed boundary conditions. Our main focus here is whether our coupled general circulation model is able to reproduce the fundamental seasonal and interannual variations in the Monsoon and the Indian Ocean Circulation. We also investigate the interactions between the Monsoon and ENSO and address the issue of Monsoon predictability.

Only a few coupled modeling studies have so far addressed these topics. Meehl (1989) investigated the results of his coupled ocean-atmosphere general circulation model in view of the importance of active ocean dynamics. However, climate drift due to the coarse ocean model resolution was significant in that particular coupled model so that the coupled general circulation model simulated a weak Monsoon. Barnett et al. (1989) studied the effect of anomalous Eurasian snow cover on regional and global climate. That study showed that the strength of the Indian Summer Monsoon is sensitive to anomalous snow cover over Eurasia, a result which was already suggested by the observational work of Hahn and Shukla (1976). Furthermore, they found also some evidence of an influence of anomalous snow cover on the ENSO cycle, but climate drift in that coupled model was also a serious problem so that this point could not be addressed adequately.

This paper is organized as follows: In section 2 we describe briefly the coupled model. Section 3 deals with the simulation of the annual cycle in both the ocean and the atmosphere, and the interannual variability is described in section 4. The main conclusions of this study are given in section 5.

## 2. Coupled model

Here we give only a brief description of the coupled general circulation model (CGCM), since it was described in more detail already in Part I of this paper. The domain of the ocean general circulation model (OGCM) extends from 70°N to 70°S and all three oceans are included. The model, however, is dynamically active only in the region 30°N to 30°S. Outside this belt, the stratification is relaxed to Levitus (1982) climatology applying a Newtonian formulation. The horizontal resolution of the OGCM was chosen in such a way that equatorially trapped waves are well resolved, with a meridional resolution of 0.5° in the region 10°N to 10°S. The meridional resolution decreases poleward and remains constant at 5° poleward of 30°. The zonal resolution is constant at 5°. In the vertical we use 17 irregularly placed levels with ten levels in the upper 300m.

The atmospheric general circulation model (AGCM) is the Hamburg version of the model of the European Centre For Medium-Range Weather Forecasts (ECMWF). It is a low order spectral model which explicitly resolves waves up to zonal wavenumber 21 (T21). The nonlinear terms are calculated on a 64 x 32 Gaussian grid which yields a horizontal resolution of about 5.6° x 5.6°. There are 19 levels in the vertical which are defined on  $\sigma$ -surfaces in the lower troposphere and on p-surfaces in the upper troposphere and stratosphere. The model includes standard physics, such as a boundary layer parameterization and interactive clouds.

The two models have been coupled without applying any correction. They exchange information over all three oceans in the region 30°N to 30°S. Outside this region boundary values are prescribed from climatology. While the AGCM is driven by the SSTs simulated by the OGCM, the OGCM is forced by the momentum, heat, and fresh water fluxes simulated by the AGCM. The coupling interval is two hours. The CGCM is forced by seasonally varying insolation. Initial conditions for the OGCM were obtained from an uncoupled 29 year control run with seasonally varying boundary forcing, whereas those for the AGCM were taken from an analysis of 1 January 1988. The coupled integration starts at January 1 and is continued for 26 years.

### 3. Annual cycle

#### 3.1 January maps

We first describe the January and July climatologies simulated by the coupled model and compare them with observations. For this purpose, long-term monthly averages were computed from the 26-year run. The observations show an almost zonal structure in sea surface temperature (SST) in January (Fig. 1a). The warmest surface waters are located predominantly south of the equator and extend to about 15°S. Typical temperatures in the warm pool are in the range from 28°C to 29°C. Poleward of 15°S the SST decreases to about 20°C near 30°S. North of the equator, the SST pattern is fairly flat with values less than 24°C only in small regions near the continents. The CGCM simulates the basic features of the January SST pattern (Fig. 1b). The warm pool, however, extends too far south and the SST south of 20°C is typically 2°C warmer than observed. This systematic bias of the CGCM is probably due to an interaction of the incoming solar radiation and the Richardson-number dependent vertical mixing scheme in the ocean. As already described in Part I, the solar radiation stabilizes the upper ocean layers in the subtropical regions, and this process cuts the vertical mixing of heat leading to a shallow warm surface layer. North of the equator, the coupled model tends to simulate too cold temperatures in the Red and Arabian Seas and south of India.

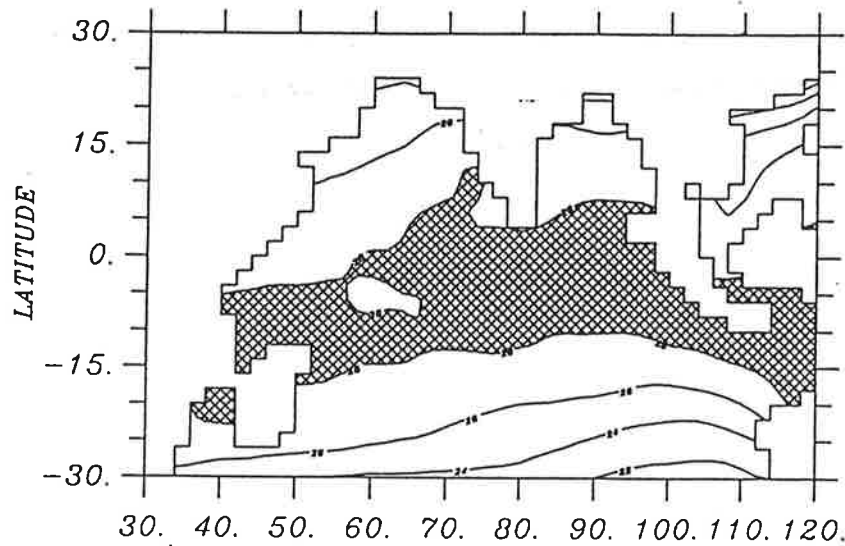
The map of climatological January wind stress as derived from the Hellermann and Rosenstein (1983) data set (Fig. 2a) is dominated by the Northeast Monsoon and the Southwest Trades which converge near 10°S. The CGCM simulates a similar wind stress pattern (Fig. 2b). The model, however, simulates the convergence zone about ten degrees too far south so that it is located near 20°S. This model deficiency is probably related to the SST error in the Southern Hemisphere described above (Fig. 1).

The climatological January rainfall (Figs. 3a and 3b) attains its maximum in the Inter-Tropical Convergence Zone (ITCZ) extending from southern Africa to the equatorial eastern Indian and western Pacific Ocean. This feature is evident in the two available climatologies (Jäger (1976) and Legates and

# Mean Climatological SST for January

## Domain: Indian Ocean

a) Observations



b) Coupled GCM

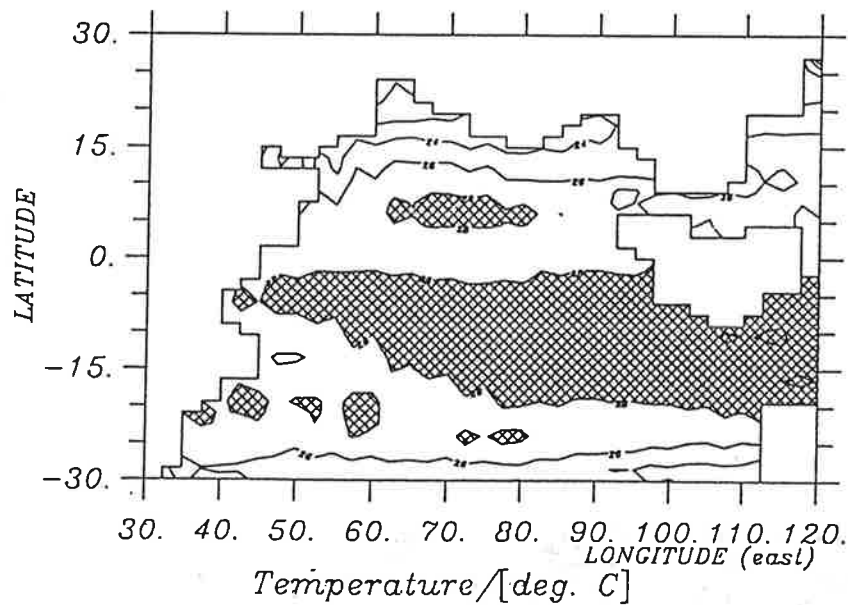


Figure 1: a) Climatological January SST [ $^{\circ}\text{C}$ ] after Levitus (1982), b) long-term mean January SST [ $^{\circ}\text{C}$ ] derived from the 26 year run with the CGCM. Shading indicates areas with SSTs of  $28^{\circ}\text{C}$  and larger.



# Climatol. Surface Wind Stress for January

## Domain: Indian Ocean

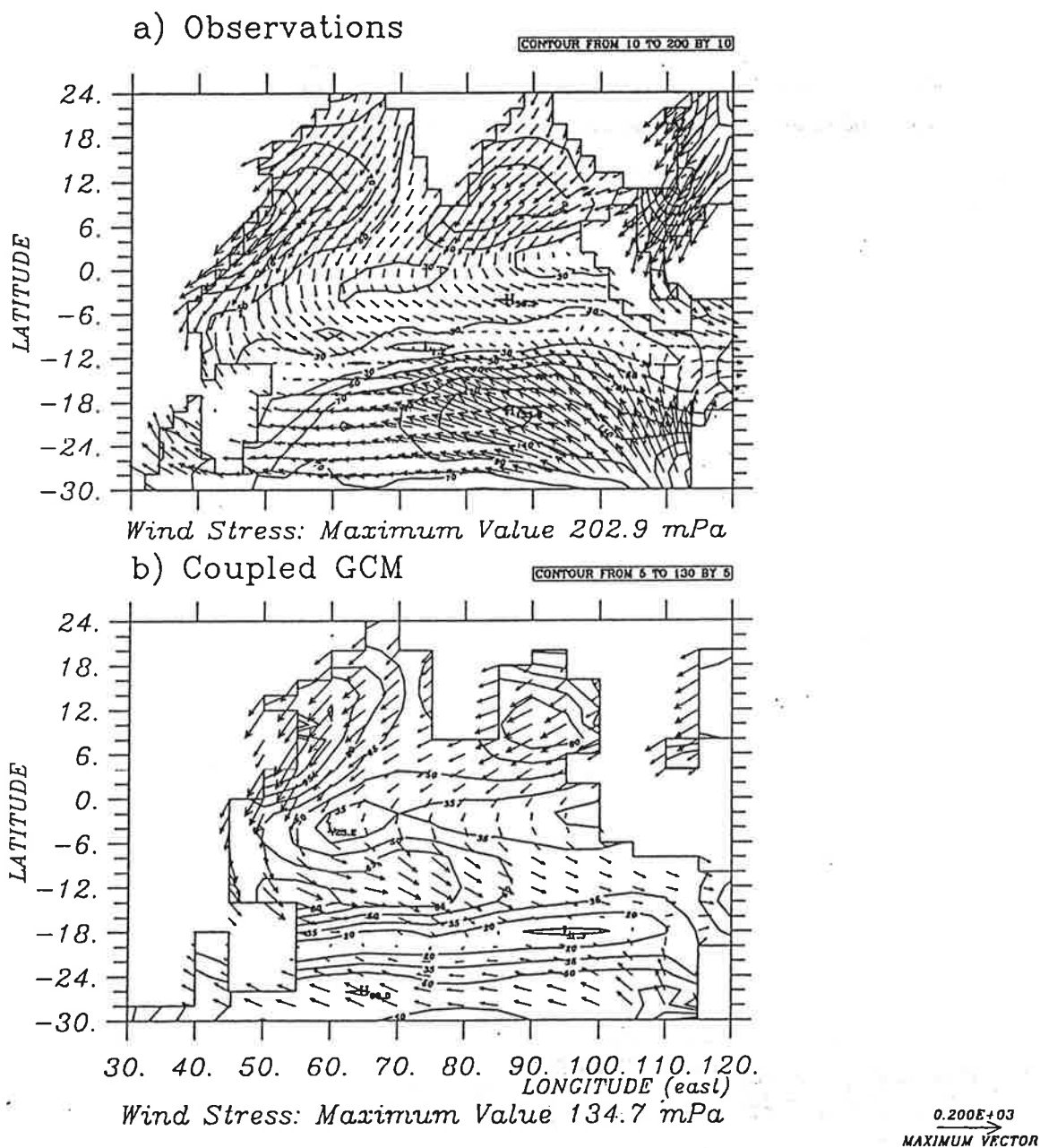
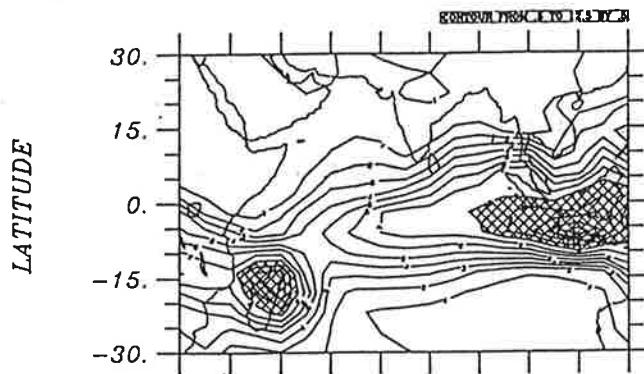


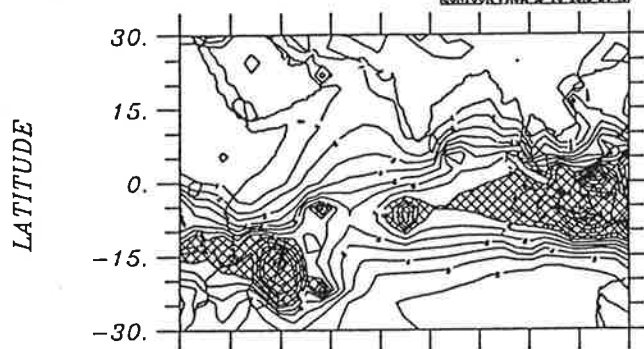
Figure 2: a) Climatological January surface wind stress [mPa] after Hellermann and Rosenstein (1983), b) long-term mean January surface wind stress [mPa] derived from the 26 year run with the CGCM.

# Climatological Precipitation for January Domain: Indian Ocean

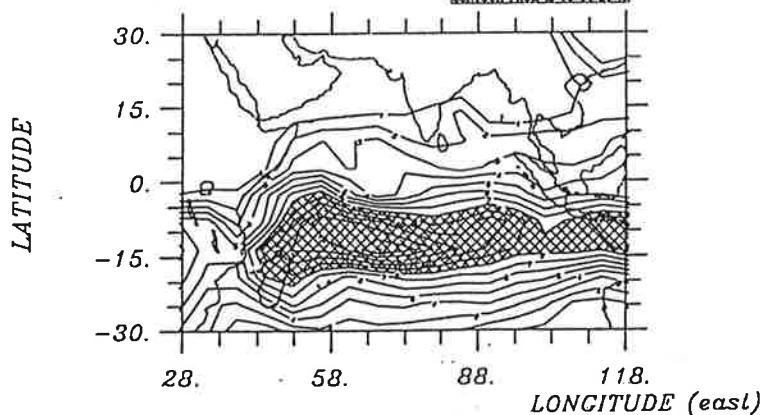
a) Observations: Jaeger



b) Observations: Legates



c) Coupled GCM



Precipitation / [mm/day]

Figure 3: a) Climatological January rainfall [mm/day] after Jäger (1976) and b) after Legates and Willmott (1990); c) long-term mean January rainfall [mm/day] derived from the 26 year run with the CGCM. Shading indicates rainfall of 8 mm/day and more.

Willmott (1990)) which are both shown in Fig. 3 to provide an indication of the uncertainty in climatological rainfall estimates. Maximum rainfall within the ITCZ is of the order of 8 mm/day. The CGCM fails to reproduce the correct orientation of the ITCZ (Fig. 3c) and simulates it as a zonal band located near 15°S. Furthermore, rainfall within the ITCZ is overestimated by the model, with typically 20% more rainfall than in the observations. The reason for the too zonal structure of the model ITCZ is the too cold western equatorial Pacific in the CGCM which forces the convection to regions off the equator (see Part I). In the Northern Hemisphere the CGCM shows no significant rainfall, in agreement with the observations.

### 3.2 June maps

The climatological June SST is characterized by uniformly warm surface waters north of the equator and a moderate meridional SST gradient in the Southern Hemisphere (Fig. 4a). The CGCM simulates a similar SST pattern (Fig. 4b). The most obvious difference between the coupled model simulation and the observations is a dipole pattern in the model SST, which consists of too cold temperatures south of India and too warm SSTs in the Bay of Bengal. This model error, however, has only a small spatial extent and is therefore unlikely to affect the large-scale atmospheric circulation.

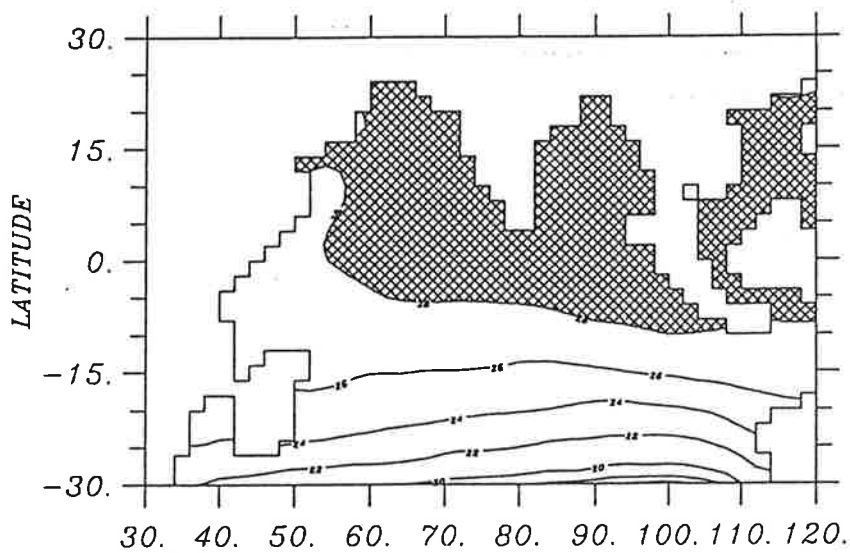
This is confirmed by the comparison of the observed with the simulated June surface stress (Fig. 5). The CGCM simulates a realistic wind stress pattern (Fig. 5b), with a pronounced South East Monsoon, which gives rise to an intense Indian Summer Monsoon rainfall (Fig. 6). However, the CGCM due to its coarse resolution is not able to reproduce the spatial details in the observed rainfall pattern, such as the minimum in rainfall over western India in the lee of the Ghats.

During the Monsoon season, the model rainfall propagates northeastward (not shown) which is in agreement with observations. The amount of rainfall and mean onset date of the model Monsoon is also in good agreement with the observations (Tables I and II). Overall, the CGCM simulates a realistic mean Monsoon given the coarse resolution of the atmosphere model (see also Fig. 9).

# Mean Climatological SST for June

## Domain: Indian Ocean

a) Observations



b) Coupled GCM

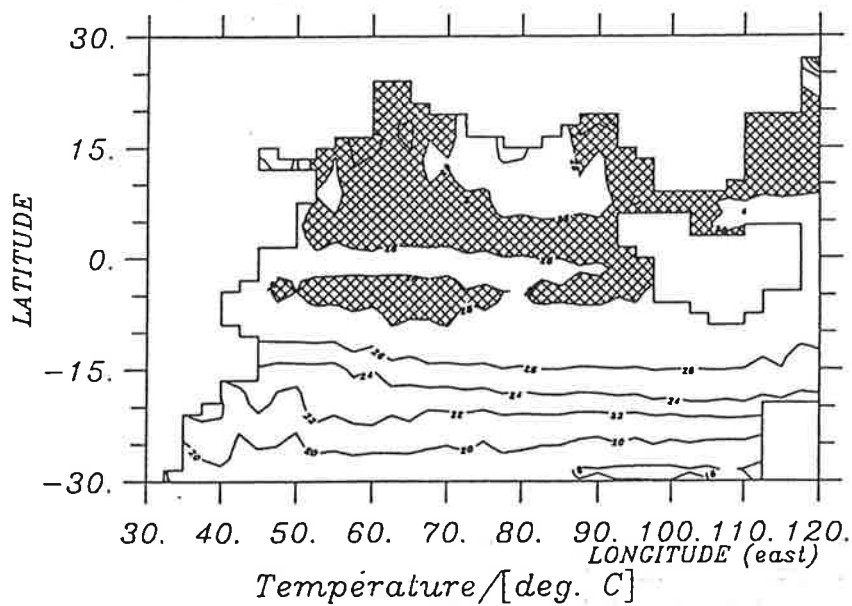


Figure 4: a) Climatological July SST [ $^{\circ}\text{C}$ ] after Levitus (1982), b) long-term mean January SST [ $^{\circ}\text{C}$ ] derived from the 26 year run with the CGCM. Shading indicates areas with SSTs of  $28^{\circ}\text{C}$  and larger.

# Climatol. Surface Wind Stress for June

## Domain: Indian Ocean

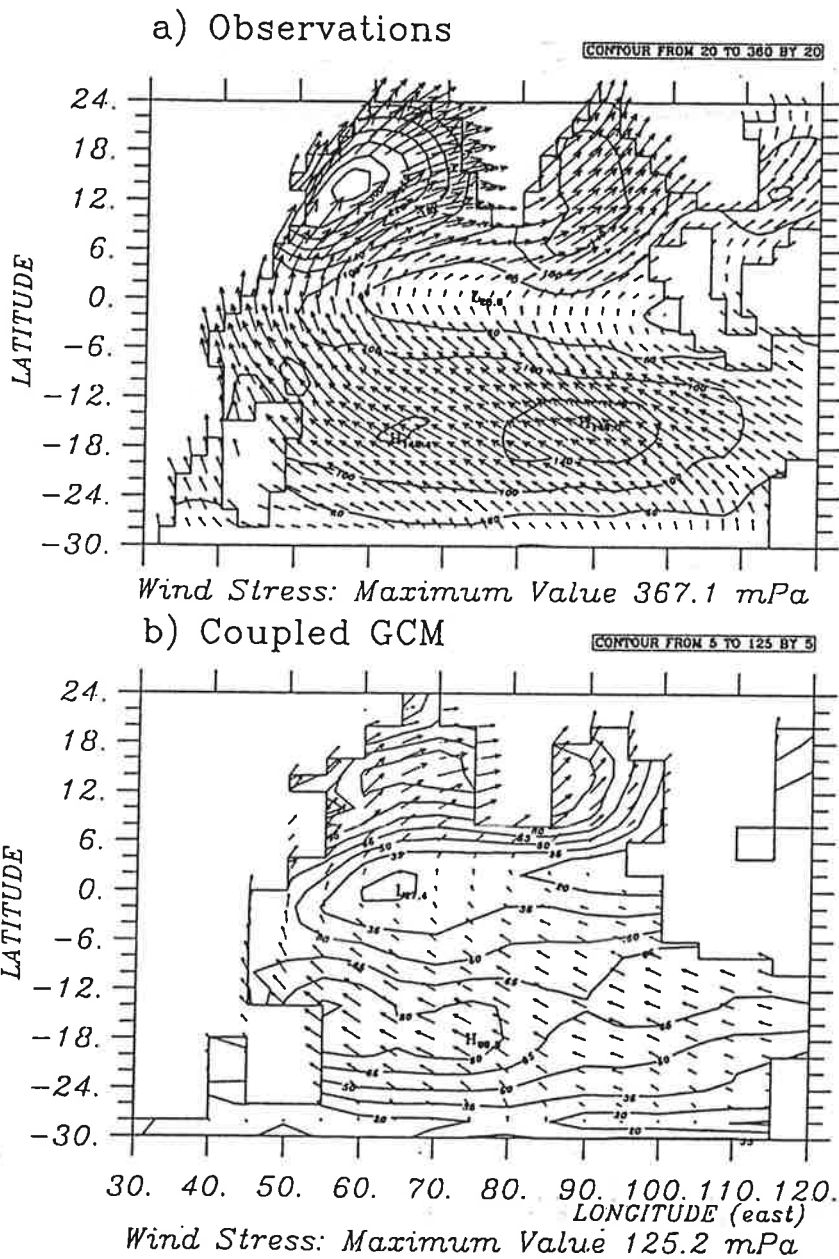
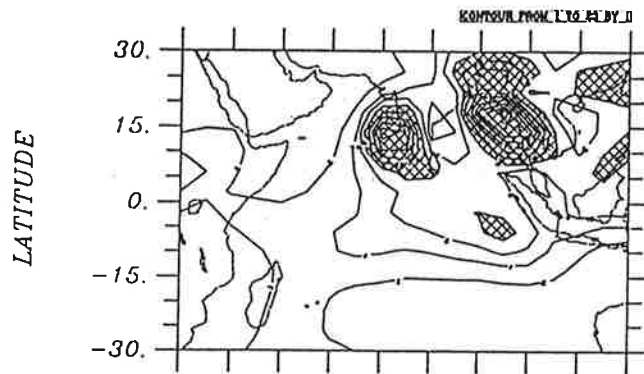


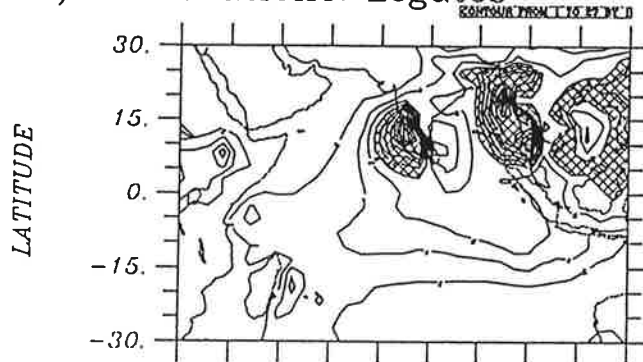
Figure 5: a) Climatological July surface wind stress [mPa] after Hellermann and Rosenstein (1983), b) long-term mean January surface wind stress [mPa] derived from the 26 year run with the CGCM.

# Climatological Precipitation for June Domain: Indian Ocean

a) Observations: Jaeger



b) Observations: Legates



c) Coupled GCM

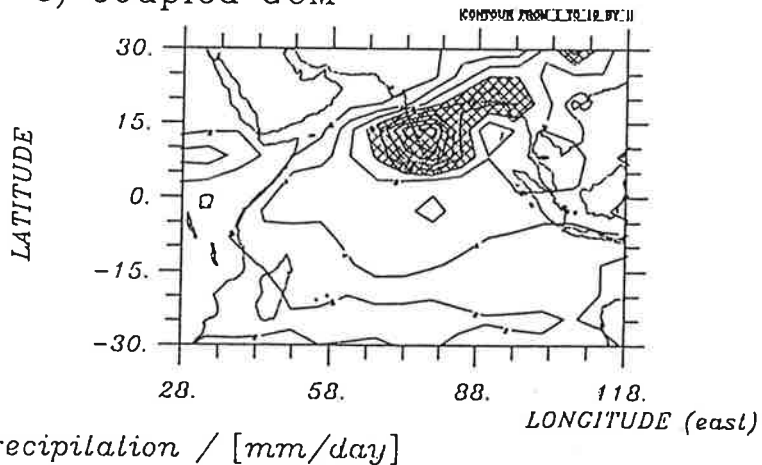


Figure 6: a) Climatological July rainfall after [mm/day] Jäger (1976) and b) after Legates and Willmott (1990); c) long-term mean January rainfall [mm/day] derived from the 26 year run with the CGCM. Shading indicates rainfall of 8 mm/day and more.

### 3.3 Temporal evolution

The Indian Ocean Circulation is characterized by rapid changes on seasonal time scales. These changes arise from large-scale air-sea-land interactions and are therefore important in verifying coupled models. One of the most interesting phenomena of the Indian Ocean Circulation is the twice-yearly occurrence of the Wyrki-Jet (Wyrki (1973)), a strong eastward flowing surface current at the equator. Although the coupled GCM simulates the two occurrences of the Wyrki-Jet, the model simulation is biased strongly toward westward currents (Fig. 7). Typical current speeds derived from observations are of the order of 60 to 80 cm/s (Reverdin (1987), Fig. 7a), whereas the model jet attains only speeds up to about 20 cm/s during spring (Fig. 7b). Furthermore, the second occurrence of the Wyrki-Jet in fall is simulated by the model only in the far eastern Indian Ocean. However, although the model shows a strong bias toward westward currents at the equator, it simulates in agreement with the observations at least a strong semi-annual cycle and westward phase propagation at the equator.

The surface current variability in the western Indian Ocean is dominated by the annual reversal of the Somali Current (Lighthill (1969)). The coupled GCM simulates this feature of the Indian Ocean Circulation reasonably well (Fig. 8). However, the coarse zonal model resolution ( $5^\circ$ ) means that boundary currents are not well resolved; thus the Somali current is simulated much too weakly by the coupled model attaining maximum speeds of only 50 cm/s, whereas observations indicate a strength of at least 100 cm/s. It should be noted, however, that a high-resolution version of the ocean component is capable of realistic simulations of the Indian Ocean Circulation when forced by observed surface wind stresses (Villwock et al. (1993)). Thus, the deficiencies described here arise either from the coarse model resolution, the climate drift of the coupled system, or a combination of both.

The annual cycle in rainfall averaged over India and Burma is shown in Fig. 9. The coupled model simulates realistically the temporal evolution of the rainfall. The maximum rainfall, however, while simulated correctly as occurring during July, is only of the order of 250 mm/day (Fig. 9b), whereas the observations indicate a peak value of about 350 mm/day (Fig. 9a). This model failure can be attributed to the atmosphere model, which yields a

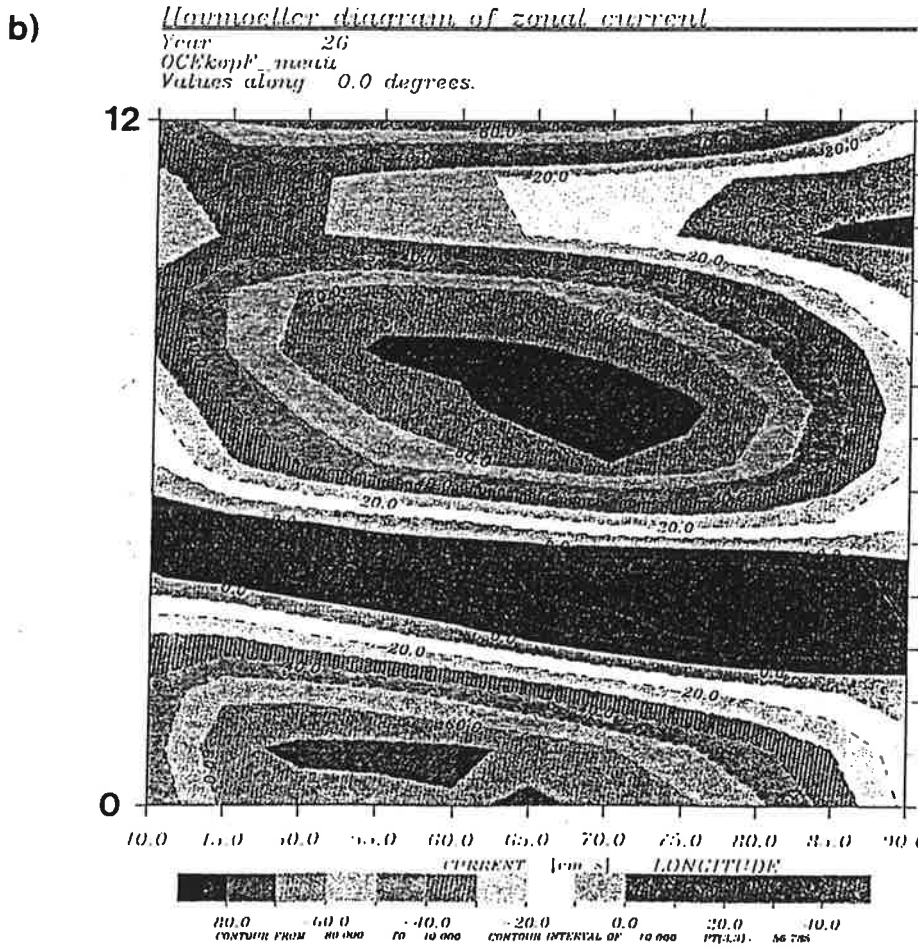
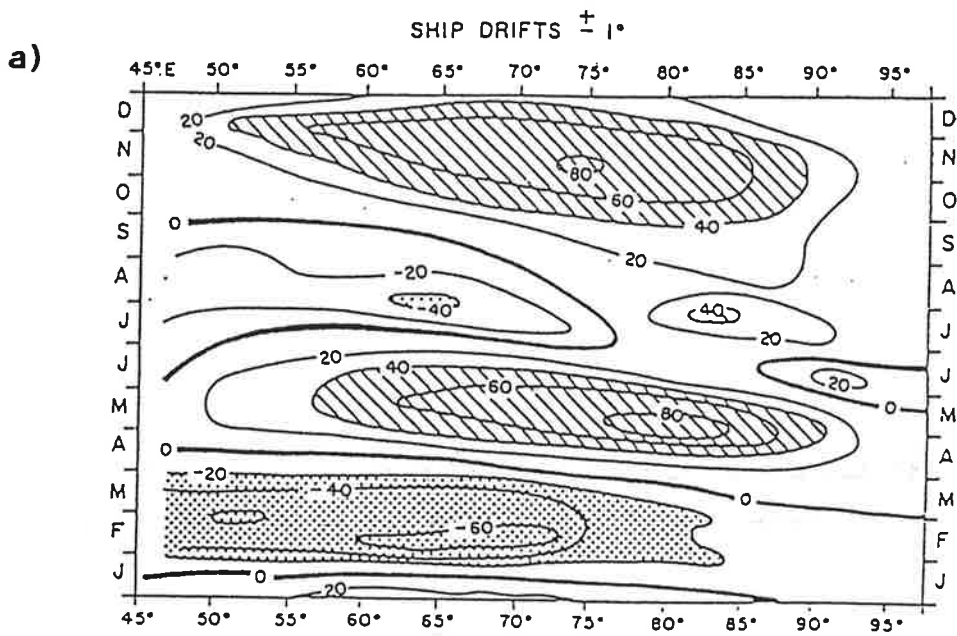


Figure 7: a) Hovmoeller diagram of climatological zonal surface currents at the equator after Reverdin, (1987), b) long-term mean zonal surface currents at the equator derived from the 26 year run with the CGCM. Units are in [cm/s].



Hovmoeller diagram of meridional current

Year 26  
OCEkopF\_meau  
Values along 0.0 degrees.

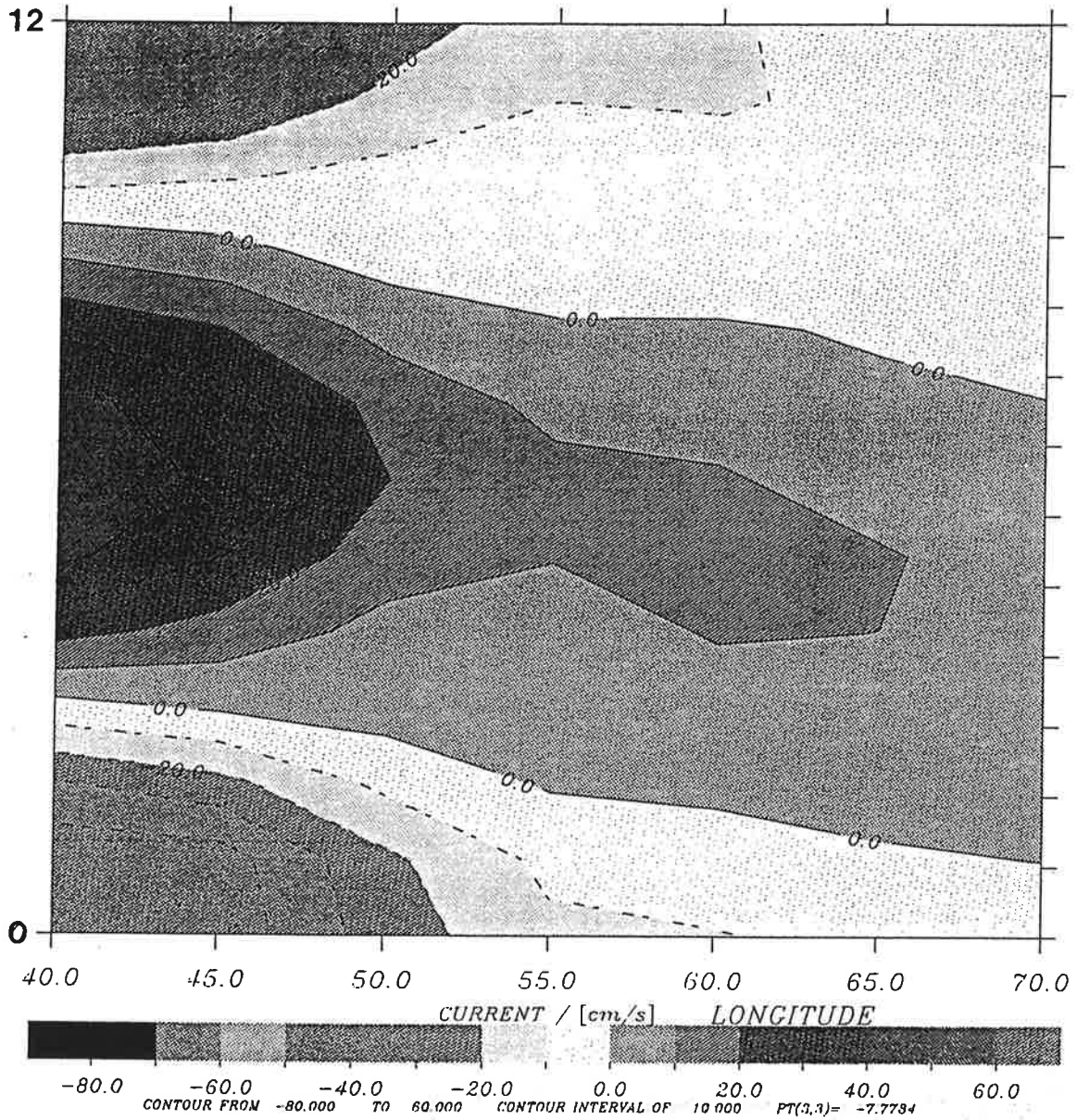
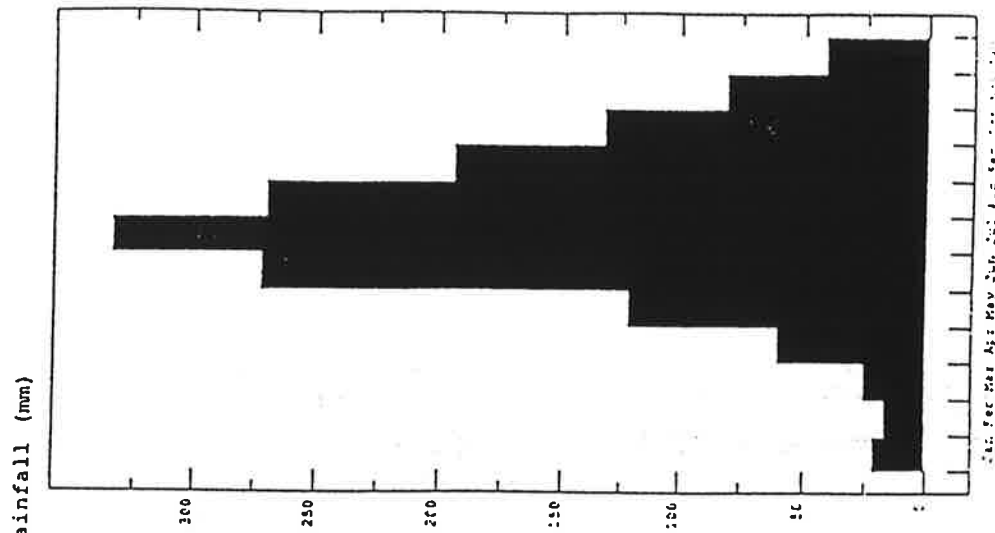
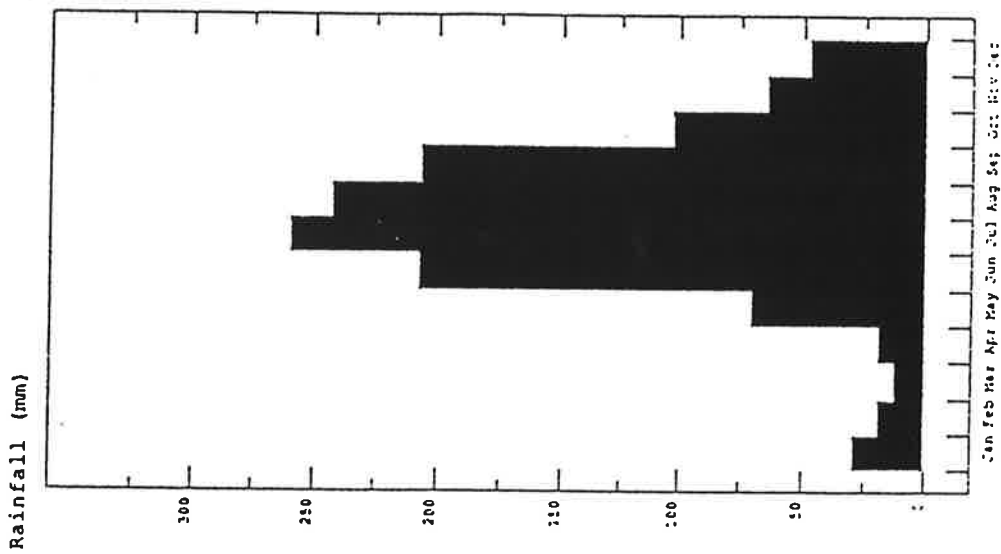


Figure 8: Hovmoeller diagram of long-term mean meridional surface currents [cm/s] at the equator derived from the 26 year run with the CGCM.

a)



b)



c)

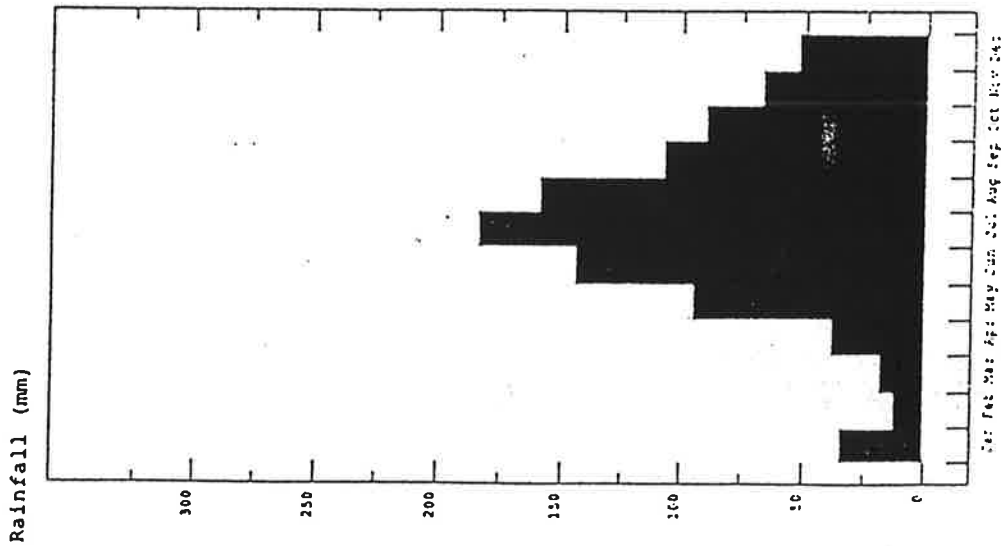


Figure 9: a) Climatological rainfall [mm/day] averaged over India and Burma as function of the calendar month after Jäger (1976), b) long-term mean rainfall [mm/day] averaged over the same region and as function of the calendar month derived from the 26 year run with the CGCM.

similar result when forced by observed SSTs (not shown). Nevertheless, overall, the coupled GCM reproduces a reasonable annual cycle in the Indian Ocean/Asian region.

#### 4. Interannual variability

Our coupled model simulates considerable variability on interannual time scales. This interannual variability, however, is mostly restricted to the Indian Ocean circulation. Typical spectra of atmospheric quantities, such as surface wind stress or heat flux over the equatorial Indian Ocean, are white. Thus, to first order, the low-frequency variability in the Indian Ocean Circulation is consistent with the 'stochastic climate model' idea of Hasselmann (1976) according to which the ocean integrates the atmospheric noise. Large-scale unstable air-sea interactions, as observed over the Pacific Ocean, are not simulated over the Indian Ocean by our coupled GCM.

One of the main questions regarding the interannual variability in the Indian Ocean/Asian region is its relationship to the El Niño/Southern Oscillation (ENSO) phenomenon. Several studies suggest that ENSO originates over the Indian Ocean and then propagates slowly eastward into the Pacific region (e. g. Barnett (1983)). We showed in Part I of this paper that, consistent with this idea and observations, our CGCM simulates a westerly wind stress anomaly over the northwestern Pacific prior to the extremes of the model-ENSO. This feature could indicate a relationship of our model-ENSO to the Indian Ocean region. We therefore investigate here the relationship between the interannual variability in the Indian Ocean/Asian region to the ENSO phenomenon.

##### 4.1 Indian Ocean response to ENSO

We applied several different statistical techniques in order to investigate whether or not interannual variability in the Pacific is forced, at least occasionally, by processes outside the Pacific. None of the results indicate that the processes in the Indian Ocean/Asian region influence significantly the ENSO cycle in the Pacific. As hypothesized by Latif et al. (1993b) the occurrence of the westerly wind stress anomaly prior to the extremes of the

ENSO cycle results from processes within the climate system over the Pacific itself and is due entirely to an anomalous meridional SST gradient near the equator.

We did find, however, a significant response of the Indian Ocean circulation to ENSO. This behaviour is best seen in a cross-spectral analysis of eastern equatorial Pacific SST anomalies (commonly expressed by the Niño-3 index, which is an area average over the region  $5^{\circ}\text{N} - 5^{\circ}\text{S}$ ,  $150^{\circ}\text{W} - 90^{\circ}\text{W}$ ) and SST anomalies averaged over the central Indian Ocean ( $2^{\circ}\text{N} - 2^{\circ}\text{S}$ ,  $70^{\circ}\text{E} - 90^{\circ}\text{E}$ ) which is presented in Fig. 10. As expected, the low-frequency variability in the Indian Ocean SST is about one order of magnitude less than that in the equatorial Pacific SST, as is clearly seen in the autospectra of the two time series (Fig. 10, upper). The squared coherence between the Indian Ocean and the Pacific SST anomalies (Fig. 10, lower) shows a pronounced maximum at a period of about 3 years, which is the preferred ENSO time scale in the coupled GCM (see Part I). The peak in the squared coherence is significant at the 95% significance level. The corresponding phase spectrum indicates a phase shift of about  $45^{\circ}$  or 5 months, with the equatorial Pacific SST anomalies leading (Fig. 10, middle). This result is also confirmed by an ordinary cross correlation analysis which shows maximum cross correlation between the two time series at a lag of 5 months. A similar lead-lag relationship is also found in observations (Villwock et al. (1993)). We note also that at very long time scales of the order of 10 years the tropical Pacific and tropical Indian Ocean vary in phase.

We carried out additionally cross spectral analyses of the Niño-3 SST anomaly time series with equatorial Indian Ocean zonal wind stress anomalies and of equatorial Indian Ocean SST with zonal wind stress anomalies averaged over the same region. These two additional cross-spectral analyses also show coherence peaks at a period of three years which are significant at the 99% and 95% level, respectively (not shown). Furthermore, the corresponding phases at this period are consistent with the idea that low-frequency changes in the Indian Ocean Circulation are forced by changes in the Pacific circulation. Thus, we conclude that the Indian Ocean responds passively to the interannual variability in the Pacific Ocean in our CGCM.

The physical processes involved in this response of the Indian Ocean SST to

NINO-3 AND T-INDIK (70E-90E,2N-2S)

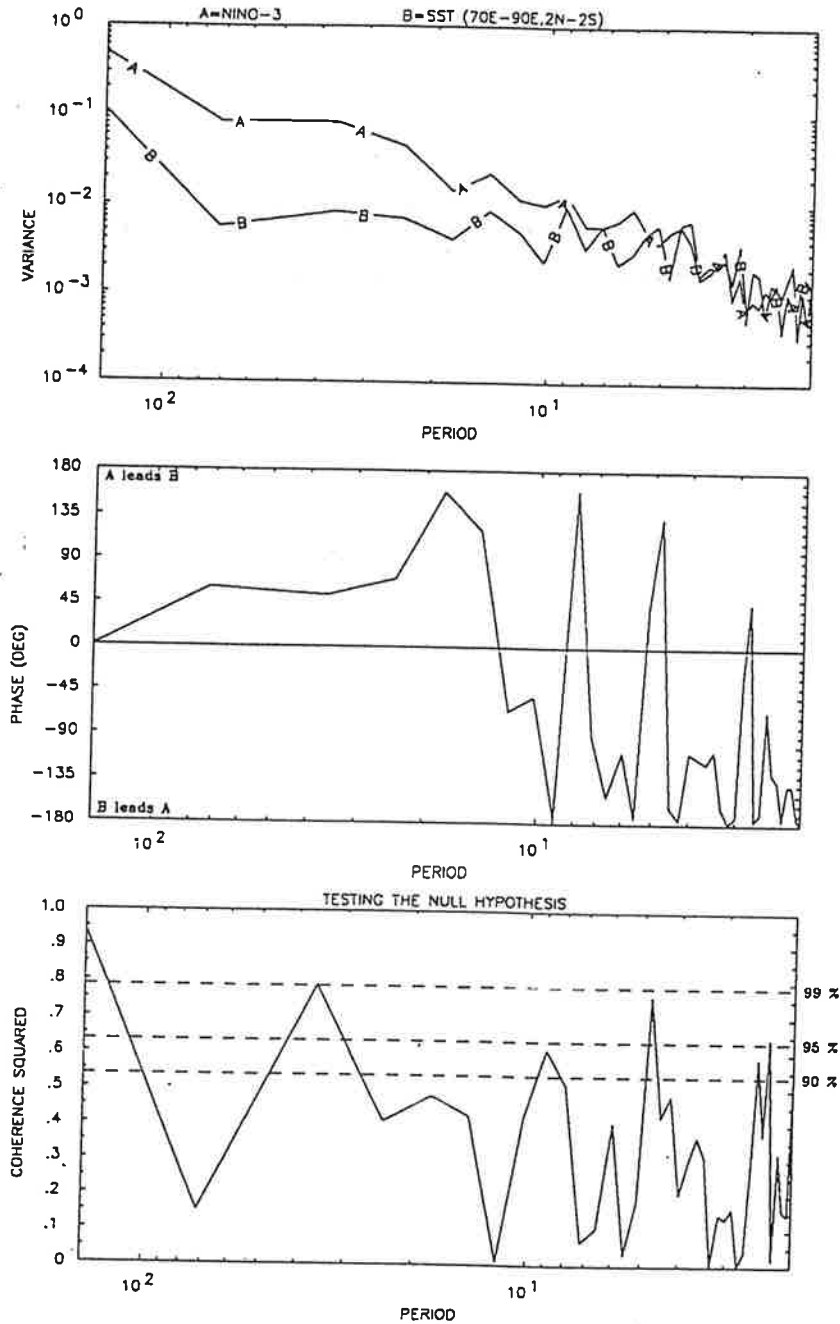


Figure 10: Cross-spectral analysis of eastern equatorial Pacific SST anomalies in the 'Niño-3' region (an area average of equatorial Pacific SST anomalies over the region  $150^{\circ}\text{W} - 90^{\circ}\text{W}$  and  $5^{\circ}\text{N} - 5^{\circ}\text{S}$ ) and central equatorial Indian Ocean SST anomalies. Upper panel: autospectra, middle panel: phase spectrum, lower panel: coherence spectrum.

ENSO are similar to those responsible for ENSO itself. This can be seen from Fig. 11 which shows the associated patterns of (low-pass filtered) equatorial Indian Ocean zonal wind stress (Fig. 11a) and SST (Fig. 11b) anomalies to the Niño-3 time series. Positive SST anomalies in the Indian Ocean are forced by westerly wind stress anomalies. Furthermore, a cross correlation analysis of Indian Ocean SST and surface heat flux anomalies (not shown) showed that the surface heat flux anomalies are out of phase with the SST anomalies so that the role of the surface heat flux is to damp the SST anomalies. Both relationships implied by our statistical analyses are found also in the Pacific (e. g. Barnett et al. (1991)). The picture derived from the coupled GCM can be summarized as follows: Once a significant SST anomaly has developed in the eastern equatorial Pacific, anomalous westerly winds develop over the equatorial Pacific and the largest portion of the equatorial Indian Ocean in response to an eastward shift of the rising branch of the Walker Circulation (Fig. 11a). The westerly wind stress anomalies over the Indian Ocean are associated with anomalous downwelling which warms the ocean's surface (Fig. 11b). Horizontal advection is unlikely to be important because of the weak horizontal SST gradients in the equatorial Indian Ocean (Figs. 1 and 4).

#### 4.2 Interannual Monsoon variability

Many studies suggest that interactions between the Monsoon and ENSO are crucial for the interannual variability in the tropical climate system (e. g. Barnett (1983)). Furthermore, there exists evidence for the Indian Summer Monsoon rainfall to be below normal during El Niños when the SST in the Pacific is anomalously high and vice versa (Shukla (1990)). We therefore investigate here, whether our CGCM is able to simulate such a relationship which would be important for successful Monsoon rainfall predictions. We first investigated observational data and computed the cross correlation between the Niño-3 SST anomaly time series and annual rainfall averaged over India and Burma. Two significant extremes in the cross correlation function are found (Fig. 12a). Niño-3 SST anomalies are negatively correlated with the rainfall during and shortly after the Monsoon season, confirming the results of Shukla (1990). The second extreme in the cross correlation function indicates that eastern equatorial SST anomalies in the fall prior to the Monsoon season are positively correlated with the rainfall anomalies during the Monsoon season. This statistical relationship is well-known (e. g. Shukla and Paolino (1983)),

# Associated Patterns to Nino3 Time Series Domain: Indian Ocean

## Zonal Wind Stress

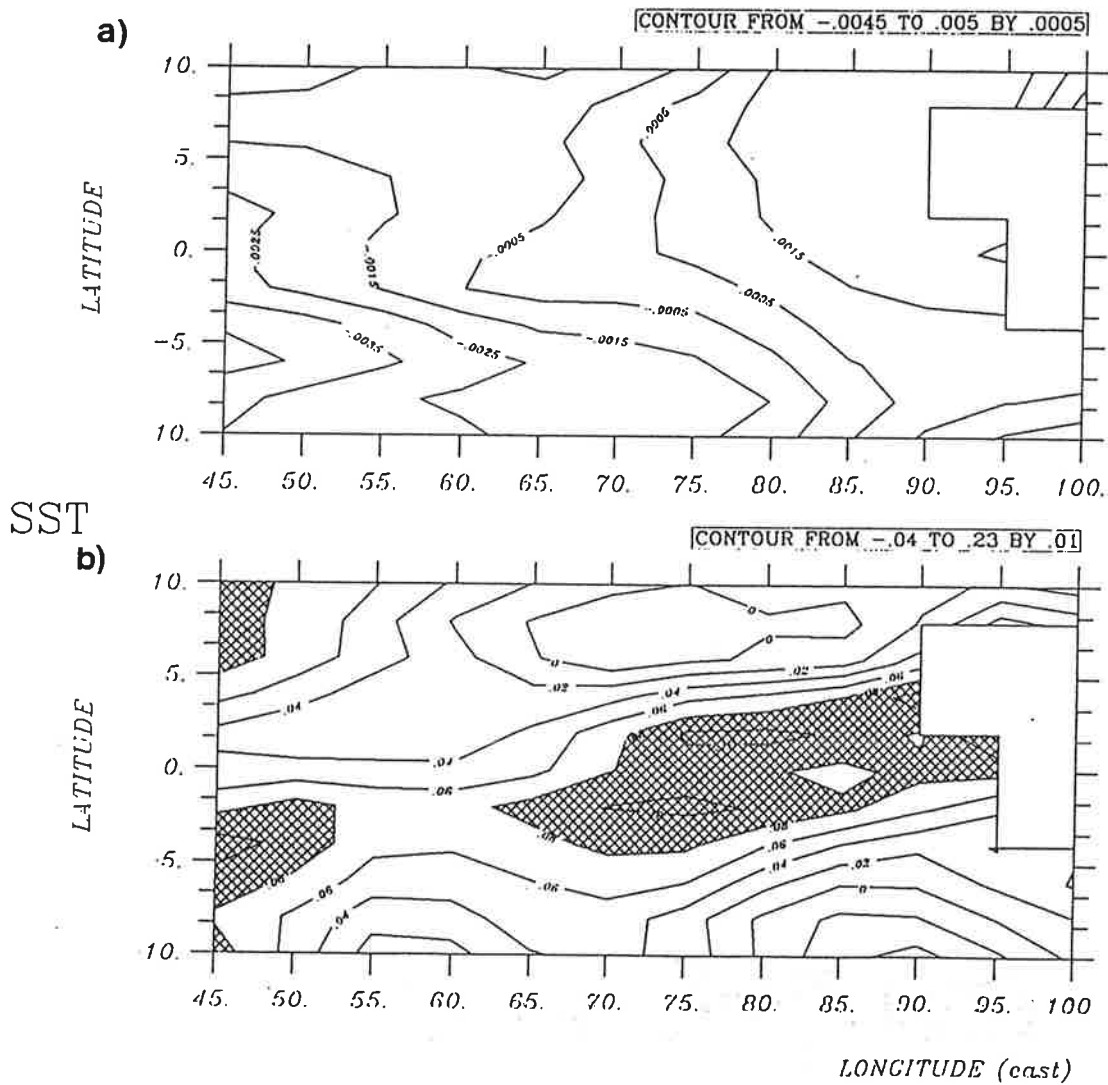
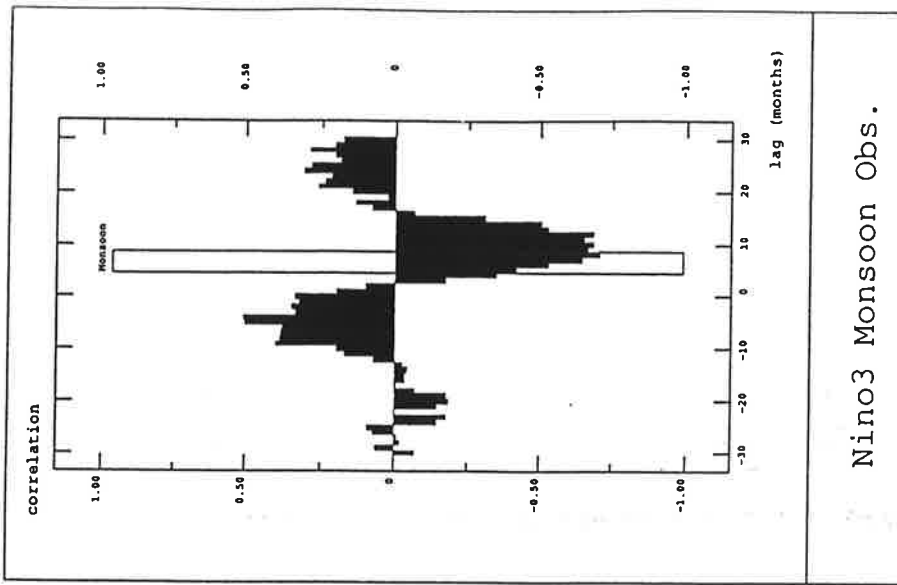
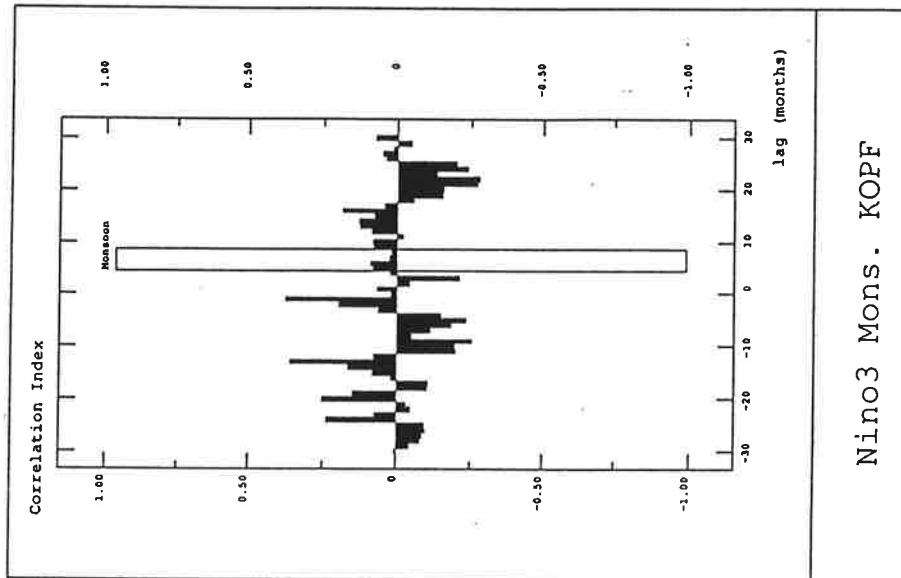


Figure 11: Associated pattern of a) equatorial Indian Ocean zonal wind stress [mPa] and b) SST anomalies [°C] to the 'Niño-3' time series.

a)



b)



c)

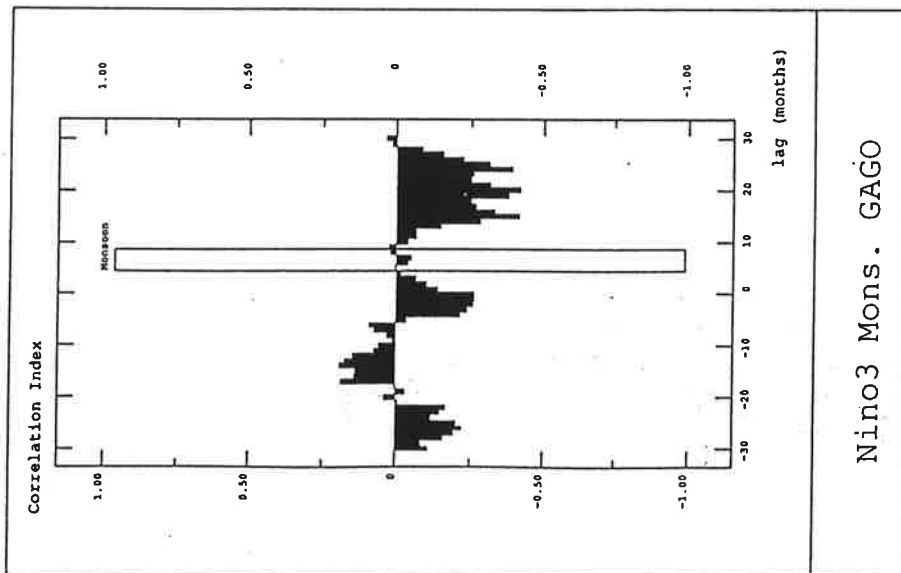


Figure 12: Cross-correlation function of Niño-3 SST anomalies with annual rainfall averaged over India and Burma as derived from a) observations, b) the 26 year run with the CGCM, and c) an uncoupled run with the AGCM forced by global observed SSTs. The time lag is in months and the bar indicates the Monsoon season.



although the physical mechanisms leading to this lead-lag relationship between Niño-3 SST and rainfall anomalies are still controversial.

We then computed the cross correlation function of Monsoon rainfall and Niño-3 SST anomalies from the output of our CGCM. The coupled model does not show any significant relationship between the two quantities (Fig. 12b). This behaviour explains why the Monsoon variability in the CGCM is considerably weaker than observed (Table 1). The model failure, however, does not affect the variability in the onset date, which is reasonably well simulated by the CGCM (Table II) and probably related to internal processes within the atmosphere itself, such as the '30-60 day oscillation' (Madden and Julian (1972)).

The question then arises, whether the lack of sufficient interannual variability in Monsoon rainfall is related to climate drift of the coupled model. In particular, the western equatorial Pacific cooled significantly during the course of the coupled integration (see Part I), which could reduce deep convection and the impact of El Niño on the global atmospheric circulation. In order to answer this question, we computed the cross correlation function for a stand-alone integration with our AGCM in which it was forced by observed near-global SSTs for the period 1970 to 1988 (details of a similar run with a slightly different cycle of our model can be found in Latif et al. (1990) and Barnett et al. (1991)). No consistent lead-lag relationship between Monsoon rainfall and tropical Pacific SST was found in this run either (Fig. 12c). Thus, either important physical processes which relate changes in SST to changes in Monsoon rainfall, such as surface land processes, are not parameterized adequately in our atmosphere model, or the resolution of the model is too coarse to allow changes in the large-scale atmospheric circulation to be reflected in rainfall.

In order to investigate the resolution dependence of the results, we also analyzed two experiments with a higher resolution version (T-42, corresponding to a horizontal resolution of about  $2.8^\circ \times 2.8^\circ$ ) of our atmosphere model in which it was forced by observed SSTs for the period 1979 to 1988. These runs were conducted as part of the Atmosphere Model Intercomparison Project (AMIP) and will be described in detail elsewhere. The two integrations differed only in the choice of the initial conditions, while the prescribed boundary conditions were identical in the two runs. The cross correlation functions between Monsoon rainfall and tropical Pacific SST computed from these runs

exhibit at least the correct shape (not shown), but the correlations were generally below the significance limits for reliable values. In particular, the two extremes during 1987 (poor Monsoon/warm tropical Pacific SST) and 1988 (good Monsoon/cool tropical Pacific SST) were simulated realistically by the T-42 model in one of the two experiments only. The correlation of Monsoon rainfall simulated between the two experiments with the T-42 model is therefore rather low at 0.38. We also computed the correlation of the zonal wind anomalies over India at the 850 hPa level between the two experiments. This correlation is also insignificant which indicates that the lower tropospheric flow over India is not determined by the boundary forcing in our experiments. On the other hand, the precipitation anomalies over the Arabian Sea were simulated almost identically in the two runs with the T-42 model, with a correlation of 0.93 between the two experiments. Large regional differences in the response characteristics over the Monsoon region were also reported by Brancovic et al. (1993), who performed ensemble integrations with the ECMWF-AGCM forced by observed SSTs.

## 5. Conclusions

We have analyzed the annual cycle and interannual variability in the Indian Ocean/Asian region simulated by a coupled ocean-atmosphere general circulation model (CGCM) in an integration of 26 years duration. We draw the following main conclusions from this study:

- 1.) The CGCM simulates realistically the annual cycle in key parameters such as Indian Ocean SST or Monsoon rainfall.
- 2.) The Indian Ocean responds passively to the ENSO-related interannual variability in the tropical Pacific. SST anomalies of the same sign as those in the Pacific are simulated in the Indian Ocean several months after SST anomalies peak in the Pacific.
- 3.) The physical processes involved in this response of the Indian Ocean circulation are related to anomalous upwelling. The surface heat flux acts as a negative feedback.

4.) The CGCM fails to simulate sufficient interannual variability in Monsoon rainfall. This failure can be traced back to the atmosphere model, which does not respond correctly to SST anomalies. This holds even at higher resolution.

5.) Monsoon predictions with our coupled general circulation model appear therefore premature.

### **Acknowledgements**

We would like to thank Dr. Klaus Arpe, Dr. Erich Roeckner and Mr. Andreas Villwock for many fruitful discussions. Many thanks also to Mrs. Marion Grunert for preparing the diagrams. This work was supported by the European Community under contract no. EV5V-CT92-0121 and by the Koerber Project. The integrations were carried out at the Deutsches Klimarechenzentrum (DKRZ).

## References

Barnett, T. P., 1983: Interaction of the Monsoon and Pacific Trade Wind system at interannual time scales. Part I: The equatorial zone. *Mon. Wea. Rev.*, 111, 756-773.

Barnett, T. P., L. Dümenil, U. Schlese, E. Roeckner, and M. Latif, 1989: The effect of Eurasian snow cover on regional and global climate. *J. Atmos. Sci.*, 46, 661-685.

Barnett, T. P., M. Latif, E. Kirk, and E. Roeckner, 1991: On ENSO physics. *J. Climate*, 4, 487-515.

Brankovic, C., T. N. Palmer, and L. Ferranti, 1993: Predictability of seasonal atmospheric variations. *J. Climate*, submitted.

Hahn, D. J. and J. Shukla, 1976: An apparent relationship between Eurasian snow cover and Indian Monsoon rainfall. *J. Atmos. Sci.*, 33, 2461-2462.

Hasselmann, K., 1976: Stochastic climate models. Part I: Theory. *Tellus*, 28, 473-485.

Hellerman, S. and M. Rosenstein, 1983: Normal monthly wind stress over the world ocean with error estimates. *J. Phys. Oceanogr.*, 13, 1093-1104.

Jäger, L., 1976: Monatskarten des Niederschlages für die ganze Erde. *Berichte des Deutschen Wetterdienstes*, 139, 1-38.

Knox, R. A., 1987 : The Indian Ocean: Interactions with the Monsoons. In: *Monsoons*, J. Fein and P. Stephens (Eds.), J. Wiley, New York, pp. 365-398.

Knox, R. A. and D. L. T. Anderson, 1985: Recent advances in the study of low-latitude ocean circulation. *Prog. Oceanogr.*, 14, 259-318.

Latif, M., J. Biercamp, H. von Storch, M. J. McPhaden, and E. Kirk, 1990: Simulation of ENSO related surface wind anomalies with an atmospheric GCM forced by observed SST. *J. Climate*, 3, 509-521.

Latif, M., A. Sterl, E. Maier-Reimer, and M. M. Junge: 1993a: Climate variability in a coupled GCM. Part I: The tropical Pacific. *J. Climate*, in press.

Latif M., A. Sterl, E. Maier-Reimer, and M. M. Junge, 1993b: Structure and predictability of the El Niño/Southern Oscillation phenomenon in a coupled ocean-atmosphere general circulation model. *J. Climate*, in press.

Legates, D. R. and C. J. Willmott, 1990: Mean seasonal and spatial variability in gauge corrected global precipitation. *J. Climatology*, 10, 111-127.

Levitus, S., 1982: Climatological atlas of the world ocean. NOAA Prof. Paper No. 13, U. S. Govt. Printing Office, Washington D. C., 173 pp., 17 microfiche.

Lighthill, M. J., 1969: Dynamic response of the Indian Ocean to onset of the Southwest Monsoon. *Philos. Trans. R. Soc. London, Ser. A*, 265, 45-92.

Luther, M. E., 1987: Indian Ocean modeling. In: *Further Progress in Oceanography*, E. Katz and J. Witte (Eds.), Nova University Press, Dania, Florida, pp. 303-316.

Madden, R. A. and P. R. Julian, 1972: Description of global-scale circulation cells in the tropics with a 40-50 day period. *J. Atmos. Sci.*, 29, 1109-1123.

Meehl, G. A., 1989: The coupled ocean-atmosphere modeling problem in the tropical Pacific and Asian Monsoon regions. *J. Climate*, 2, 1146-1163.

Meehl, G. A., 1992: Effect of tropical topography on global climate. *Annu. Rev. Earth Planet. Sci.*, 20, 85-112.

Neelin, J. D., M. Latif, M. A. F. Allaart, M. A. Cane, U. Cubasch, W. L. Gates, P. R. Gent, M. Ghil, C. Gordon, N. C. Lau, C. R. Mechoso, G. A. Meehl, J. M. Oberhuber, S. G. H. Philander, P. S. Schopf, K. R. Sperber, A. Sterl, T. Tokioka, J. Tribbia, S. E. Zebiak, 1992: Tropical air-sea interaction in general circulation models. *Climate Dynamics*, 7, 73-104.

Reverdin, G., 1987: The upper equatorial Indian Ocean: The climatological seasonal cycle. *J. Phys. Oceanogr.*, 17, 903-927.

Shukla, J., 1990: Short term climate variability and predictions. Conference volume, Second World Climate Conference, Geneva, Switzerland, 29 October - 2 November, 1990.

Shukla, J. and D. A. Paolino, 1983: The Southern Oscillation and long-range forecasting of the summer monsoon rainfall over India. *Mon. Wea. Rev.*, 111, 1830-1837.

Villwock, A., M. Latif, and E. Maier-Reimer, 1993: Indian Ocean response to El Niño. *J. Geophys. Res.*, in prep.

WMO, 1992: Simulation of interannual and intraseasonal Monsoon variability. Report of workshop, National Center for Atmospheric Research, Boulder, Colorado, U. S. A., 21.-24. October, 1992. World Climate Research Programme, WCRP-68, WMO/TD No. 470, Geneva, Switzerland.

Wyrtki, K., 1973: An equatorial jet in the Indian Ocean. *Science*, 181, 262-264.

## Tables

Table 1

	rainfall [mm]	std [mm]	std [%]
observations	1067	137	13
CGCM	950	66	7
uncoupled AGCM	932	76	8

Table 1: Monsoon rainfall statistics (mean and standard deviation) derived from observations, the coupled general circulation model (CGCM), and the uncoupled atmospheric general circulation model (AGCM) forced by observed SSTs. Rainfall was averaged over India and Burma.

Table 2

	onset day	std [days]
observations	1 st June	7.7
CGCM	3 rd June	6.4
uncoupled AGCM	2 nd June	10.0

Table 2: Monsoon onset date statistics (mean and standard deviation) derived from observations, the coupled general circulation model (CGCM), and the uncoupled atmospheric general circulation model (AGCM) forced by observed SSTs. Rainfall was averaged over India and Burma. The Monsoon onset is defined as the date at which a rainfall of 3 mm/day is exceeded.